High Pressure Research: An International Journal

Publication details, including instructions for authors and subscription information:
http://www.tandfonline.com/loi/ghpr20

Synthesis and characterization of the new high pressure phases $ACu_3V_4O_{12}$(A=Gd, Tb, Er)

N. V. Melnikova [a] , N. I. Kadyrova [b] , I. S. Ustinova [a] , Ya. Yu. Volkova [a] , A. P. Tyutyunnik [b] , Yu. G. Zaynulin [b] , A. N. Babushkin [a] & A. V. Korolev [c]

[a] Low Temperature Physics Department , Ural Federal University , Ekaterinburg , Russia

[b] Institute of Solid State Chemistry , Urals Branch of Russian Academy of Sciences , Ekaterinburg , Russia

[c] Institute of Metal Physics , Ural Branch of Russian Academy of Sciences , Ekaterinburg , Russia

Published online: 29 Apr 2013.

To cite this article: N. V. Melnikova , N. I. Kadyrova , I. S. Ustinova , Ya. Yu. Volkova , A. P. Tyutyunnik , Yu. G. Zaynulin , A. N. Babushkin & A. V. Korolev (2013) Synthesis and characterization of the new high pressure phases $ACu_3V_4O_{12}$(A=Gd, Tb, Er), High Pressure Research: An International Journal, 33:2, 418-424, DOI: 10.1080/08957959.2013.788695

To link to this article: http://dx.doi.org/10.1080/08957959.2013.788695

High Pressure Research, 2013
Vol. 33, No. 2, 418–424, http://dx.doi.org/10.1080/08957959.2013.788695

Taylor & Francis
Taylor & Francis Group

Synthesis and characterization of the new high pressure phases $A\mathrm{Cu_3V_4O_{12}}(A = \mathrm{Gd, Tb, Er})^{\dagger}$

N.V. Melnikova[a]*, N.I. Kadyrova[b], I.S. Ustinova[a], Ya.Yu. Volkova[a], A.P. Tyutyunnik[b], Yu.G. Zaynulin[b], A.N. Babushkin[a] and A.V. Korolev[c]

[a]*Low Temperature Physics Department, Ural Federal University, Ekaterinburg, Russia;* [b]*Institute of Solid State Chemistry, Urals Branch of Russian Academy of Sciences, Ekaterinburg, Russia;* [c]*Institute of Metal Physics, Ural Branch of Russian Academy of Sciences, Ekaterinburg, Russia*

(*Received 31 August 2012; final version received 15 March 2013*)

New $A\mathrm{Cu_3V_4O_{12}}$ (A = Gd, Tb, Er) phases have been prepared at high pressure and high-temperature conditions ($P \sim 8$–9 GPa, $T \sim 1000$°C) in a toroid-type high pressure cell. These compounds crystallize in the cubic symmetry with a perovskite-like structure. At ambient pressure, they are paramagnetic and have activation-type conductivity. The effect of high pressure (10–50 GPa) on the electrical properties of the materials was analyzed in the temperature range from 78 to 300 K. Pressure ranges of the transition from activation type to metallic conductivity have been determined. The crystal structure of $A\mathrm{Cu_3V_4O_{12}}$ (A = Gd, Tb, Er) was found to be stable up to 50 GPa.

Keywords: synthesis; perovskite-like structure; high pressure; electrical properties; impedance spectroscopy

1. Introduction

Studies of perovskite-family compounds with the general formula $[AC_3](B_4)\mathrm{O_{12}}$ are of interest both from the fundamental and applied viewpoints since these materials exhibit different types of magnetic ordering, giant dielectric permittivity, magnetoelectric effect, as well as high-temperature superconductivity and colossal magnetoresistance. [1–3] The description of the mechanisms explaining the transport properties of $[AC_3](B_4)\mathrm{O_{12}}$ and their correlation with the structure is an actual problem. The aim of this work is to synthesize, certify, and study the properties of the new high pressure perovskite-like phases $A\mathrm{Cu_3V_4O_{12}}$ (A = Gd, Tb, Er) in a wide temperature and pressure ranges, as well as to study stability of the structure up to 50 GPa.

2. Experimental

Thermobaric synthesis was performed in a toroid-type high pressure cell following the technique described in detail elsewhere. [4] Appropriate mixtures of $\mathrm{Gd_2O_3}$, $\mathrm{Dy_2O_3}$, $\mathrm{Tb_4O_7}$, $\mathrm{V_2O_5}$, $\mathrm{Cu_2O}$,

*Corresponding author. Email: nvm.melnikova@gmail.com
[†]This paper was presented at the Lth European High Pressure Research Group (EHPRG 50) Meeting at Thessaloniki (Greece), 16–21 September 2012.

Table 1. Synthesis conditions and unit cell parameters of $ACu_3V_4O_{12}$ compounds ($A = Gd$, Tb, Er).

	Synthesis conditions			Unit cell spacing
Compound	P (GPa)	T (°C)	t (min)	(Å)
$Gd_{0.73}Cu_3V_4O_{12}$	9	1000	10	7.2939(2)
$Tb_{0.7}Cu_3V_4O_{12}$	9	1000	10	7.2918(5)
$Er_{0.73}Cu_3V_4O_{12}$	8	1000	30	7.2853(5)

and Cu were used for the synthesis. The synthesis conditions (Table 1) were chosen so as to prepare the single-phase materials.

X-ray powder diffraction patterns were collected on a STADI – P automatic diffractometer (STOE, Germany). X-ray diffraction experiments at high pressures were carried out on a special diffractometer consisting of a high-flow X-ray generator FR-D, a focusing optical system Flux Max, and a Bruker APEX CCD detector at the Institute of Geochemistry and Geophysics, University Bayreuth (Germany), in a high pressure cell with diamond anvils. The diffraction data were analyzed by the Rietveld method using the GSAS software. [5,6] The morphology of the obtained samples and their chemical composition were studied using a JEOL-JSM 6390 LA scanning electron microscope equipped with a JED-2300 X-ray microanalyzer.

The temperature dependence of magnetic susceptibility was measured on a SQUID magnetometer MPMS-5-XL (Quantum Design) in magnetic field 1 kOe. To apply the high pressure conditions, rounded cone–plane-type diamond anvil cells (DAC) were used. Anvils of carbonado-type artificial diamonds with good conductivity make it possible to examine the electrical properties of samples placed into DAC. [7] A low-temperature press was used, which ensures pressure variation in the temperature interval from 4.2 to 400 K. The method for pressure estimation and DAC calibration is described in detail in works. [8,9] The studied samples with a diameter of ~0.2 mm and thickness from 10 to 30 μm were obtained by compression in DAC of the initial powdered materials. The electrical properties (impedance, admittance, tangent of loss angle, or loss tangent) were examined at ambient pressure and at 10–50 GPa in alternating current in the frequency range from 200 Hz to 200 kHz using the impedance spectroscopy method, as well as measurements of the resistance were performed on a direct current. The impedance technique is one of the extensively used approaches for studying the electrical properties of heterogeneous materials (in DAC at pressures above 10 GPa, the sample is not homogeneous for various reasons – appearance of mixtures of phases, deviations from the hydrostatic nature of pressure in the sample bulk, etc.), which allows the contributions associated with electrical conduction of different phases, interfaces, electrode processes, electric polarization in the bulk, measuring cell, etc. to be distinguished from the material's response to the external electric field. [10,11]

3. Results and discussion

The compounds $ACu_3V_4O_{12}$ (A = Gd, Tb, Er) crystallize in the cubic system (sp. gr. $Im\bar{3}$, $Z = 2$) with a perovskite-like structure (Table 1, for the structure representation see [12]). The results of the crystal structure refinement for $Gd_{0.73}Cu_3V_4O_{12}$ are listed in Table 2. Experimental, calculated, and difference X-ray powder diffraction patterns are shown in Figure 1. Selected bond lengths (cation–anion) and bond angles (cation–anion–cation) are listed in Table 3.

All $ACu_3V_4O_{12}$ compounds (A = Gd, Tb, Er) have positive magnetic susceptibility χ. The temperature dependence of magnetic susceptibility for $Er_{0.73}Cu_3V_4O_{12}$ (Figure 2(a)) is well described in the framework of the Curie–Weiss law. The Curie constant, C, is 0.0112 K cm^3/g for the $Er_{0.73}Cu_3V_4O_{12}$ and 0.00751 K cm^3/g for $Gd_{0.73}Cu_3V_4O_{12}$. For $Er_{0.73}Cu_3V_4O_{12}$, the effective

Table 2. Structural and isotropic thermal parameters for $Gd_{0.73}Cu_3V_4O_{12}$.

Atom	Position	x/a	y/b	z/c	U_{iso}•100 (Å^2)	Fraction
Gd	2a	0	0	0	3.6(2)	0.802(4)
Cu	6b	0	0.5	0.5	3.1(1)	1.0
V	8c	0.25	0.25	0.25	2.9(1)	1.0
O	24g	0	0.3008(5)	0.8182(5)	2.2(1)	1.0

Note: The refined formula is $Gd_{0.802(4)}Cu_3V_4O_{12}$.

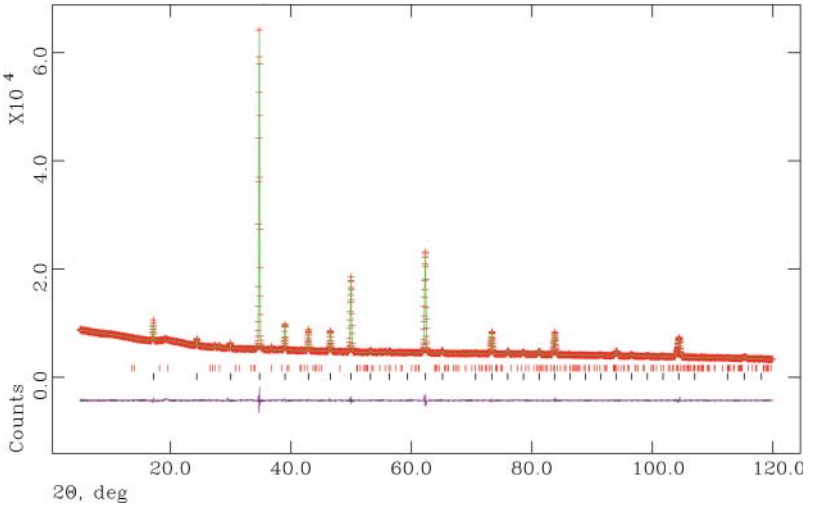

Figure 1. Experimental (+), theoretical (solid line), as well as line diagrams and difference diagrams for $Gd_{0.73}Cu_3V_4O_{12}$.

Table 3. Shortest interatomic distances and bond angles in $Gd_{0.73}Cu_3V_4O_{12}$.

Distances (Å)			Bond angles (°)		Bond angles (°)	
Gd–O	12×	2.565(4)	V–Gd–O	37.55(3)	Gd–V–O	54.23(9)
Mean		2.565	V–Gd–O	101.27(4)	Gd–V–O	125.77(9)
Expected		2.487[a]	V–Gd–O	142.45(3)	O–V–O	90.7(2)
			O–Gd–O	116.28(3)	O–V–O	89.3(2)
Cu–O	4×	1.968(2)	O–Gd–O	62.31(9)		
Mean		1.968	O–Gd–O	63.72(3)	Gd–O–Cu	106.5(2)
Expected		1.954	O–Gd–O	117.69(9)	Gd–O–V	88.2(1)
					Cu–O–V	108.43(6)
V–O	6×	1.9268(7)	O–Cu–O	84.8(3)	V–O–V	142.4(1)
Mean		1.9268	O–Cu–O	95.2(3)		
Expected		1.960				

[a]Expected distances are calculated with oxidation states corresponding to $Gd^{3+}_{0.802}[Cu^{2+}_{2.594}Cu^{1+}_{0.406}]V^{4+}_4O^{2-}_{12}$ and ionic radii from Shannon [13].

moment μ_{ef} is estimated to be $7.99\mu_B$, the Weiss constant (Θ) is negative, and its calculated value is 19 K, which indicates the antiferromagnetic interaction between magnetic moments of erbium ions.

Analysis of the frequency dependencies of impedance, admittance, the loss tangent allowed obtaining ranges of frequencies which characterize the properties of the samples and where the influence of the electrode processes can be ignored. The temperature and baric dependencies of the electrical properties were measured in these frequency ranges. The temperature dependencies

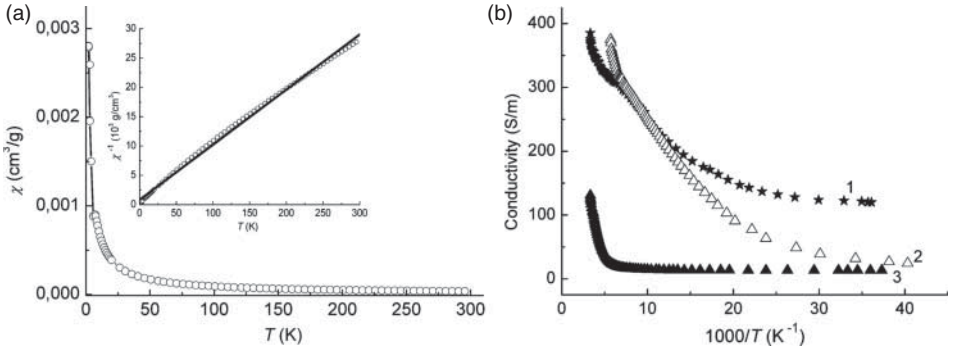

Figure 2. (a) Temperature dependencies of magnetic susceptibility χ and reciprocal susceptibility $1/\chi$ (inset) for $Er_{0.73}Cu_3V_4O_{12}$at ambient pressure. (b) Temperature dependencies of conductivity for $Gd_{0.73}Cu_3V_4O_{12}$ (1), $Er_{0.73}Cu_3V_4O_{12}$ (2), and $Tb_{0.7}Cu_3V_4O_{12}$ (3) at ambient pressure.

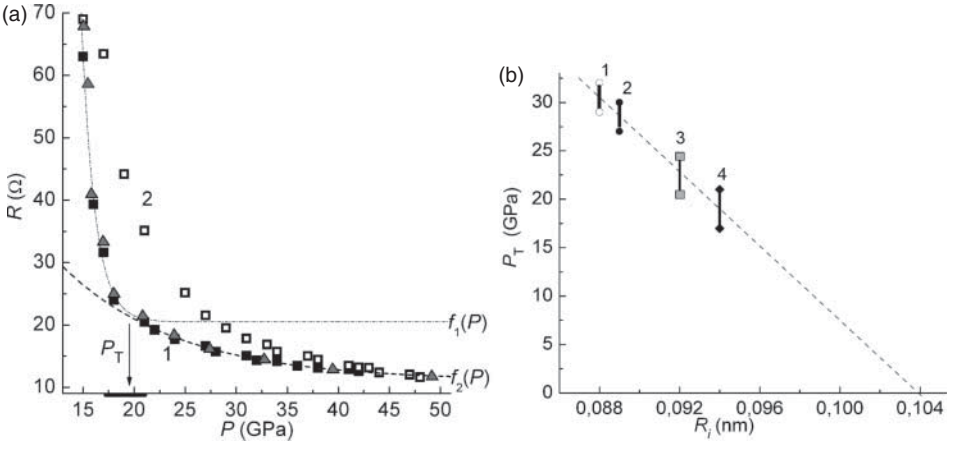

Figure 3. (a) Pressure dependencies of electrical resistance of $Gd_{0.7}Cu_3V_4O_{12}$ when the pressure increases (1) or decreases (2) at room temperature, squares – the first pressure cycle, triangles – the second pressure cycle. The dashed lines indicate the functions $f_1(P)$ and $f_2(P)$ approximating the dependence $R(P)$ when the pressure increases in the ranges $P < 16$ GPa and $P > 21$ GPa, respectively. P_T is the pressure, at which a transition from one to another type of $R(P)$ dependence takes place. (b) Pressure intervals P_T of considerable changes in the behavior of electrical characteristics of $ACu_3V_4O_{12}$at room temperature: $Tm_{0.75}Cu_3V_4O_{12}$ (1) is given for comparison, $Er_{0.73}Cu_3V_4O_{12}$ (2), $Tb_{0.7}Cu_3V_4O_{12}$ (3), and $Gd_{0.7}Cu_3V_4O_{12}$ (4) – as functions of the ionic radius R_i of A (ionic radii according to Shannon [13]). The presumable type and features of the high pressure crystal structure can be predicted by extrapolation of the data presented in this figure to the region of zero (atmospheric) pressure and by comparison with the structure (at atmospheric pressure) of an analogous compound, in which the ionic radius of lanthanide A^{3+} is 0.103–0.105 nm, for example, compounds with Ce or La.

of conductivity at ambient pressure point to the activation character (Figure 2(b)). Analysis of the effect of high pressures (up to 50 GPa) in a wide temperature range on the electrical properties of materials allowed us to define the pressure intervals, where the behavior of loss tangent, impedance, admittance, and electrical resistance change essentially. Electrical resistance of the examined compounds measured at room temperature decreases when the pressure is raised from 10 to 50 GPa. The pressure dependencies of electrical resistance $R(P)$ can be approximated into two pressure intervals by two exponential functions with different exponents (Figure 3(a)). [12] As the pressure grows, the resistance falls rapidly first, and then the rate of the resistance reduction decreases abruptly. The logarithm of resistance is an almost linear function of pressure in the two pressure intervals. The ranges of pressures P_T, at which a transition from one type of the

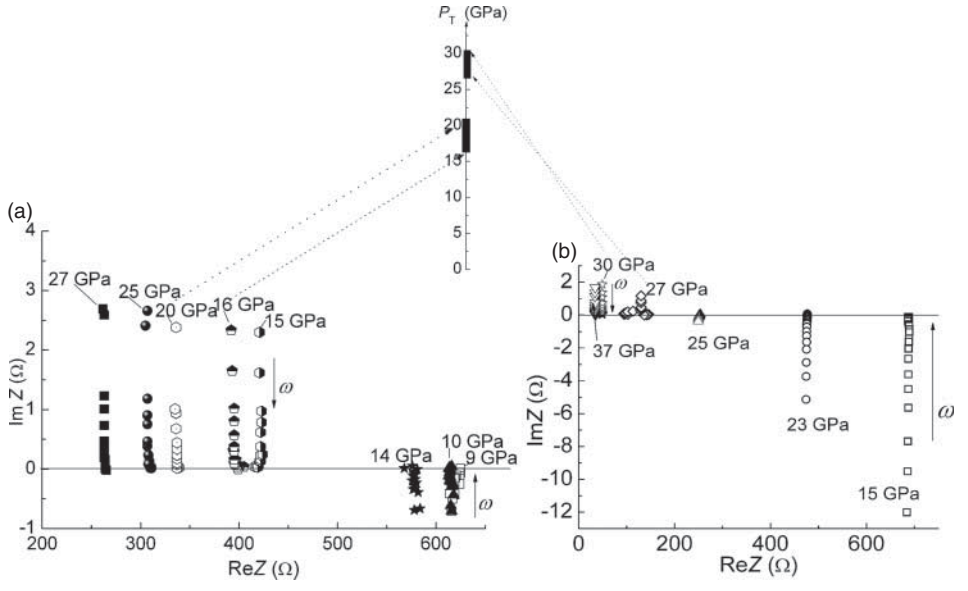

Figure 4. The hodographs of the impedance of the cell with $Gd_{0.7}Cu_3V_4O_{12}$ (a) and $Er_{0.73}Cu_3V_4O_{12}$ (b) at fixed pressures (when pressure increases). The solid arrows show the direction of a frequency increase. Dotted arrows show the pressures which belong to P_T ranges (Figure 3(b)). The pressure range where the imaginary part of the impedance reverses sign corresponds to the most rapid decrease of the resistance with pressure increase (see Figure 3(a) for $Gd_{0.7}Cu_3V_4O_{12}$).

$R(P)$ dependence to another takes place, are presented in Figure 3(b). Here, an effect of chemical compression becomes apparent, which explains the displacement of the pressure interval, where the behavior of electrical characteristics of $Gd_{0.73}Cu_3V_4O_{12}$, $Tb_{0.7}Cu_3V_4O_{12}$, and $Er_{0.73}Cu_3V_4O_{12}$ changes appreciably, to higher pressures. The loss tangent, the imaginary parts of the impedance, and of the admittance reverse their signs in the pressure intervals 14–15 and 25–27 GPa for the compounds $Gd_{0.73}Cu_3V_4O_{12}$and $Er_{0.73}Cu_3V_4O_{12}$, respectively (Figure 4 demonstrates the behavior of the impedance). These pressure intervals precede P_T ranges. This may suggest that at high pressures electric dipoles or complexes are formed or change, whose presence and behavior evoke this response of the system to the alternating electric field. [14] When the pressure decreases from maximum to atmospheric values, the changes in the loss tangent, impedance, and admittance behavior repeat in the reverse order. In the pressure ranges corresponding to these transitions and in P_T ranges, we have examined the temperature dependencies of the electrical resistance of the materials (Figure 5). At atmospheric pressure, all the examined compounds exhibit activation-type conductivity, the values of activation energy are typical of oxides that are intrinsic semiconductors and are equal to 0.03, 0.06, and 0.05 eV for $Gd_{0.73}Cu_3V_4O_{12}$, $Tb_{0.7}Cu_3V_4O_{12}$, and $Er_{0.73}Cu_3V_4O_{12}$, respectively. When the pressure increases, the temperature dependencies of resistance exhibit qualitatively similar changes. At fixed pressures in the P_T range and in the pressure range where the imaginary parts of the impedance and of the admittance reverse their signs, the $R(T)$ dependencies exhibit maxima corresponding to the transition from the semi-conducting to metallic dependence of the resistance at the corresponding temperatures. These features of $R(T)$ in the above-mentioned pressure ranges may be due to existence of a mixture of phases (metallic and semiconductor) because of different compressibilities of the polyhedra (such as AO_{12} and VO_6) in the perovskite-like structure and due to changes in the electronic structure with pressure increase. The presence of the hysteresis in the pressure dependence of the resistance with pressure increase and pressure decrease (Figure 3(a)) supports this assumption. At pressures above the upper limit of the P_T range, the $R(T)$ dependence is of a metallic character.

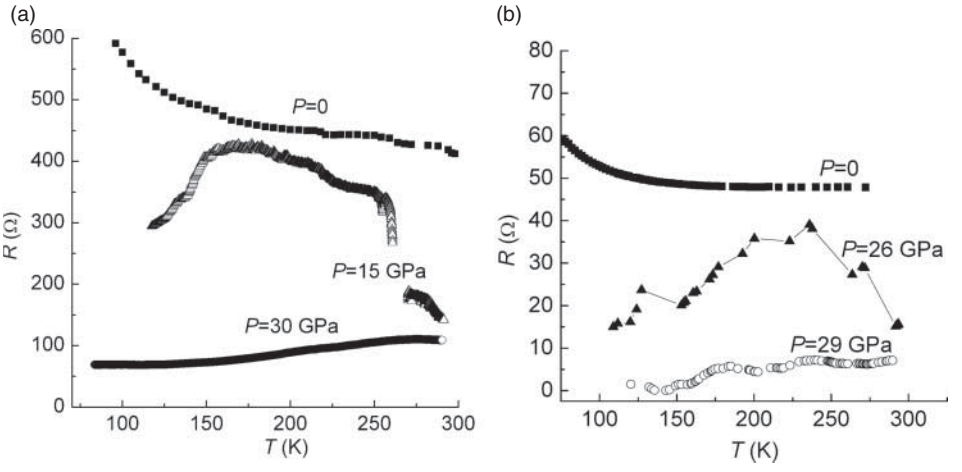

Figure 5. Temperature dependencies of resistance for $Gd_{0.7}Cu_3V_4O_{12}$ (a) and $Er_{0.73}Cu_3V_4O_{12}$ (b) at fixed pressures.

For the compounds $[AC_3](B_4)O_{12}$ with a perovskite-like structure, it is typical that at external pressures the *B*–O–*B*-bond angle φ increases and the width of the charge carrier band grows, whose value is proportional to $\cos^2 \varphi$. [15] In the considered compounds, when the external pressure increases, the V–O–V-bond angle φ may grow (in the examined compounds at ambient pressure $\varphi \sim 142 - 143°$), the deformation of VO_6 octahedra takes place, the width of the conduction band increases, additional electron carriers appear, and electrical resistance decreases. The transition from one to another type of pressure dependence of resistance, each of which can be described, for example, by exponential functions with different exponents (Figure 3(a)) can be due to reversible distortions of the crystal structure and to the variations in the electronic structure. When the pressure decreases, all the changes in the resistance are reversible. The features of the electronic states and magnetic interactions in the perovskite-like phases $ACu_3V_4O_{12}$ are determined primarily by the states of vanadium and copper sublattices and by their interaction with the oxygen sublattice [16] and, consequently, by the transition from the activation-type to metallic-type dependence of conductivity when the pressure increases. Analysis of the effect of high pressures on the crystal structure of $Er_{0.73}Cu_3V_4O_{12}$ confirmed, as expressed in [12], the supposition that the structure of the compounds is distorted without fundamental restructuring when the pressure increases; this is also supported by the behavior of electrical parameters when the pressure decreases (the electrical parameters return to the values typical of the materials before pressure was applied, and here a hysteresis is observed). The lines on the X-ray diffraction pattern of $Er_{0.73}Cu_3V_4O_{12}$ obtained at 27.8 GPa (belonging to the P_T range) correspond to the cubic structure and are shifted toward higher angles relative to those recorded at ambient pressure. Thus, the crystal system remains cubic, and the lattice parameters decrease. When the unit cell volume of $Er_{0.73}Cu_3V_4O_{12}$ decreases by 7% ($a = 7.2853(5)$ Å at ambient pressure and $a = 7.109(5)$ Å at 27.8 GPa), conductivity increases by a factor of 15–20, and the temperature dependence of the conductivity becomes a metallic type. Analogous changes in the resistance are observed with an increase in pressure for all the examined compounds having an activation dependence of resistance at ambient pressure. This behavior of the electrical characteristics (considering the low values of activation energies) is typical for semi-metals and agrees with the conclusion [16] that at ambient pressure $ErCu_3V_4O_{12}$ is a semi-metal. In work [16], the electronic structure of $ErCu_3V_4O_{12}$ is studied with the use of the projected augmented wave method, and electron–electron correlations are taken into consideration in the calculations. Thus, the studies of the effect of high pressures (10–50 GPa) at temperatures between 78 and 300 K on the electrical properties of high pressure

perovskite-like phases $ACu_3V_4O_{12}$ (A = Gd, Tb, Er) allowed us to determine the pressure ranges of the transition from activation-type to metallic-type conductivity. Since the electrical properties are very sensitive to crystal structure changes, the behavior of the electrical characteristics of the $ACu_3V_4O_{12}$ compounds at varying pressure may attest that the crystal structure of the perovskite-like phases is stable in the considered pressure range.

4. Conclusion

In summary, the new phases $ACu_3V_4O_{12}$ (A = Gd, Tb, Er) with a perovskite-like structure have been synthesized at high pressures and high temperatures. Their crystal structures have been determined and described. At ambient pressure, these materials are paramagnetic and have activation-type conductivity. The effect of high pressures (up to 50 GPa) on the structure and properties of these materials has been analyzed.

Acknowledgements

The work was supported by the Russian Foundation for Basic Research (RFBR grants Nos 10-03-00163-a and 12-02-31607) and partially by the Ural Federal University Development Program for financial support of young scientists. The authors are grateful to Prof L.S. Dubrovinsky, University Bayreuth (Germany) for the possibility to conduct high pressure X-ray measurements.

References

[1] Zeng Z, Greenblat M, Subramanian MA, Croft M. Large low-field magnetoresistance in perovskite-type $CaCu_3Mn_4O_{12}$ without double exchange. Phys Rev Lett. 1999;82:3164–3167.
[2] Subramanian MA, Sleight AW. $ACu_3Ti_4O_{12}$ and $ACu_3Ru_4O_{12}$ perovskites: high dielectric constants and valence degeneracy. Solid State Sci. 2002;4(3):347–351.
[3] Vasil'ev AN, Volkova OS. New functional materials. Vestnik RFFI. 2008;3:29–53.
[4] Kadyrova NI, Zaynulin YuG, Volkov VL, Zakharova GS, Korolev AV. High-pressure defect phase $Ce_xCu_3V_4O_{12}$. Russ J Inorg Chem. 2008;53(10):1542–1545.
[5] Toby BH. EXPGUI, a graphical user interface for GSAS. J Appl Crystallogr. 2001;34:210–213.
[6] Larson AC, Von Dreele RB. General Structure Analysis System (GSAS). Los Alamos (New Mexico): Los Alamos National Laboratory; 2004. Report No.: Los Alamos National Laboratory Report LAUR 86-748.
[7] Vereshchagin LF, Yakovlev EN, Vinogradov BV, Stepanov GN, Bibaev KKh, Alaeva TI, Sakun VP. Megabar pressure between anvils, High Temp-High Press. 1974;6:499–504.
[8] Babushkin AN. Electrical conductivity and thermal EMF of CsI at high pressures. High Press Res. 1992;6:349–356.
[9] Babushkin AN, Kandrina YA, Schkerin SN, Volkova YY, Kheifets OL. Phase transitions and metastable states. In NATO APW – frontiers of high pressure research II: application of high pressure to low-dimensional novel electronic materials, Vol. 146; Dordrecht: Kluwer Press; 2001. p. 131–141.
[10] Mases M, You S, Weir ST, Evans WJ, Volkova Ya, Tebenkov A, Babushkin AN, Vohra YK, Samudrala G, Soldatov AV. In situ electrical conductivity and Raman study of C_{60} tetragonal polymer at high pressures up to 30 GPa. Phys Status Solid B. 2010;11–12:3068–3071.
[11] Kandrina YuA, Babushkin AN. High-pressure electrical properties of CdS studied by impedance spectroscopy. Inorg Mater. 2008;5:457–459.
[12] Melnikova NV, Kadyrova NI, Ustinova IS, Zainulin YuG, Babushkin AN. Effect of high pressures on the electrical properties of the perovskite-like phases of $ACu_3V_4O_{12}$. Bull Russ Acad Sci Phys. 2012;76(3):321–324.
[13] Shannon RD. Revised effective ionic radii and systematic studies of interatomic distances in halides and chalcogenides. Acta Crystallogr. 1976;A32:751–767.
[14] Kadyrova NI, Melnikova NV, Ustinova IS, Babushkin AN, Korolev AV, Zaynulin YuG. Synthesis and properties of high-pressure phase $[Er_xCu_3](V_4)O_{12}$. Bull Russ Acad Sci Phys. 2009;73(11):1539–1541.
[15] Golosova NO, Kozlenko DP, Savenko BN, Voronin VI, Glazkov VP. The influence of high pressure on the crystal and magnetic structures of the $La_{0.7}Sr_{0.3}CoO_3$ cobaltite. Phys Solid. 2006;48(1):96–101.
[16] Petrik MV, Medvedeva NI, Kadyrova NI, Zainulin YuG, Ivanovskii AL. Effect of electron correlations on the electronic structure and magnetic properties of the perovskite-like high-pressure phase $ErCu_3V_4O_{12}$. Phys Solid. 2010;52(8):1709–1713.